

Inference About Functional Connectivity From Multiple Neural Spike Trains

Zhanwu Liu

February 16, 2011

Abstract

In neuroscience study, it is desirable to understand how the neuronal activities are associated and how the association changes with time based on multiple spike train recordings from multielectrode array. The term functional connectivity is used to describe the association between neurons and the change of association with task purpose. In this proposed thesis, I will study the statistical details of functional connectivity inference. First, the preliminary results show the effect of sample size, connection strength and basis set on functional connectivity inference, I would like to explore further for large networks so that I can estimate the sample size needed for functional connectivity inference; secondly, I will explore the models and algorithms being used for inference, and the current plan is to combine two families of methods, i.e. point process-generalized linear model based methods and graph theory based methods, to develop procedure that can be used to infer functional connectivity network given limited amount of data; finally, I will explore the possible information we can obtain when the sample size is too small to infer functional connectivity reliably.

1 Introduction

The advance of multielectrode arrays make it possible that dozens or even hundreds of neurons can be recorded at the same time, and it is expected that the number of simultaneous recorded neuron will increase to thousands in the near future [1]. On one hand, this advance in data recording technology makes it possible to study one of the most interesting questions of neuroscience, i.e. how neurons interact with each other to represent and process information. On the other hand, several challenges exist [2]. First, the length of recording session is usually limited by the animal conditions. This limit of the amount of available data makes the inference

more difficult when the number of parameters increase. Secondly, the computational cost increases at fast pace with the increase of number of neurons recorded. While the number of neurons being considered increase linearly with the number of recorded neurons, the number of pairwise interaction terms increase quadratically.

In computational neuroscience, *functional connectivity* describes the correlated behavior between neural elements of different levels, such as different cortex regions, neuron populations or individual neurons [3]. It has been shown that neurons work together to represent and transfer information, for example, a neuron in the primary visual cortex (V1) will only respond to the stimulus in a specific region of the visual field (known as receptive field), but at the same time, stimulus outside of the receptive field can modulate this response [4]. In addition, it has been shown that the connectivity changes over different conditions [5]. In application, when connectivity information was included in decoding, the decoding error can be greatly reduced [6]. Because understanding functional connectivity is important in both the appreciation of the mechanism of neural systems and the application of neuroscience, a lot of research efforts have been devoted to functional connectivity study.

In the past decade we observed fast progress in the study of functional connectivity. In the early years, studies focused on descriptive measures such as correlation or coherence measure [7], joint peristimulus time histogram (JPSTH) [8]. Recently, a family of methods based on point process-generalized linear model (GLM) were developed to take into account the coupling between neurons [9, 10, 11]. In these models, a temporal coupling function between neurons is estimated, and this function represents the connection between neurons. Point process-GLM provided a principled framework for statistical estimation, such that we can understand the details of how one neuron affects another.

We also observed the use of graph theoretical methods in the study of functional connectivity [12, 13, 14]. Graphical models can not only provide a good summary by visualization of the inferred functional connectivity network, but also help us infer the functional connectivity network directly [13]. In the past years, different methods have been developed for network and/or complex systems, which can help us model network dynamics from network topology, understand the robustness of network information representation [12], and decode the neural signal by identifying the important neurons in the network.

The above mentioned two families of methods have different advantages and disadvantages. The point process-GLM methods provided details of interneuronal connections that can be used to explain the spiking events of the target neuron, but the connection may not be meaningful because there are other explanations for the connection, such as common input [15]. On the other hand, graphical models can provide good visualization of the connectivity pattern, can rule out the correlation

caused by common input and indirect connection. In addition, some collective behavior can be explained by the network as a whole only but not the individual neurons [16]. However the detail of the connection is usually not available for the graph theoretical models [14].

My goals in this proposed thesis include:

- Understand the factors affecting functional connectivity inference with point process GLM methods, including sample size, coupling strength and basis functions.
- Develop new methods for functional connectivity inference by combining point process GLM methods with graph theoretical methods.
- Apply the newly developed method to real data. Several different sets of data will be considered.
- Explore possible useful information about functional connectivity from data with less than ideal sample size.

2 Literature Review

2.1 The concept of functional connectivity

2.1.1 Related concepts

It is well-known that in the brain, different neural units work together to process and transfer information. The coordination between neural units has been observed at different levels: different brain regions, different clusters of neurons in one region, or different neurons in the local neural circuit [3]. One of the basic goal of neuroscience research is to infer how these neural units connect with each other, how do they work together and how the relationship changes when the task changes. To describe the connectivity between neural units, several different concepts were used when the connectivity was viewed from different perspective [17].

Anatomic connectivity describes the physical (synaptic) connection between neurons, which is usually difficult to observe. The only organism with complete neuron connection map is the nematode *C. elegans* [18] because it has only 302 neurons. A term *connectome* proposed by Olaf Sporns et.al. [19] to describe a long term goal of obtaining connectivity information for human brain. In the paper the authors acknowledged that it is nearly impossible to obtain the human neuron map technically because there are about 10^{10} neurons and 10^{13} connections in the cortex only. In addition, it is not necessary to obtain such a map because the connections

may change rapidly (plasticity), and the change in single synapses usually has no macroscopic effect.

Functional connectivity describes the statistical relationship between different neural units. However, the exact meaning of functional connectivity was interpreted differently by different researchers. It was initially defined as temporal coherence or correlation among the activity of different neural units [8, 17, 20]. Latterly another definition based on statistical dependency was proposed for the neuroimaging community [21]. In more recent works on functional connectivity study, usually the ability of one unit being used to predict another one was used, for example, see [9, 15, 22].

Effective connectivity defines the cause and effect relationship between neural units. Despite its seemingly obvious relationship with anatomic connectivity, effective connectivity is not a unique statement about anatomic connectivity because the arrangement of neurons lead to the same overall behavior is not unique [23]. Instead a definition being accepted by many researchers is: *effective connectivity is the simplest neuron-like circuit that would produce the same temporal relationship as observed experimentally between two neurons in a cell assembly* [8, 20].

From the descriptions above, it is clear that the three different concepts are closely related. For example, anatomical connectivity based on synaptic connection will lead to functional and causal connectivity; on the other hand, it is also possible that anatomical connectivity be modulated by functional connectivity [24]; if the firing event of one neuron causes the firing event of another (effective connectivity), we should expect to see functional connectivity between these two neurons; and if two neurons are connected by synapse, it is likely to observe causal relationship between the two. The three concepts are being used at different levels of neural system organization. In the following sections I will focus on the microscopic level, i.e. the connectivity between neurons within a neuron circuit.

2.1.2 Sources of functional connectivity

It is commonly believed that the correlated activity between neurons may come from three different sources [7]. First it is possible that two neurons have direct (monosynaptic) connection; secondly, the two neurons may have indirect (polysynaptic) connection; and thirdly when two neurons share a common input or encode the same information, correlated behavior can also be observed. The inference of functional connectivity is made more complicated by the different sources. For example, Vidne[15] et. al. showed that when common input was included explicitly in the model, no interaction terms can be observed in the retinal ganglion cells. One of the goals of functional connectivity study is to distinguish the different situations.

2.2 Functional connectivity and point process GLM framework

2.2.1 Parallel spike trains are modelled as interacting point processes

The neurons transfer information through action potentials, or spikes. An action potential is a short lasting event (usually < 1 ms) during which the membrane potential of a neuron rises and falls, usually follows a typical shape. It is believed that the exact shape of an action potential contains no information, it is the time when the action potential happens contains all the information. Thus a series of spikes from one neuron, also known as spike train, can be represented by a list of spike times (t_1, t_2, \dots, t_n) .

The natural model for the spike train is point process [25]. Given an observation interval $(0, T]$, a point process records the event (spike) times. To characterize a point process, usually the conditional intensity function $\lambda(t|H(t))$ is used, which is defined as

$$\lambda(t|H(t)) = \lim_{\Delta \rightarrow 0} \frac{P[N(t + \Delta) - N(t) = 1|H(t)]}{\Delta}$$

where $N(t)$ is a counting measure denotes the number of spikes in the interval $(0, t]$, and $H(t)$ denotes the spiking history up to time t .

The conditional firing rate $\lambda(t|H(t))$ is usually represented as function of spiking history, ensemble as well as the external stimuli [10], as shown below.

$$\log \lambda_i(t|H(t)) = \log \lambda_{i0} + h_i(t|H(t)) + \sum_{j \neq i} f_{ji}(t|H(t)) + s_i(x(t))$$

where λ_{i0} is the base firing rate of unit i , h_i is the contribution from the history of unit i , f_{ji} is the contribution from unit j to unit i , and s_i is the contribution from external stimulus $x(t)$.

The log-likelihood function of a Poisson process can be written as [26, 27]

$$\log L(t_1, \dots, t_n) = \sum_{i=1}^n \log \lambda(t_i) - \int_0^T \lambda(t) dt$$

And the parameters can be fitted by maximizing the likelihood function [26, 9] or by Bayesian methods [28].

2.2.2 Modelling of interaction between neurons in the point process GLM framework

In the point process GLM framework, the interaction between neurons are described by the ensemble terms f_{ji} as shown above, and the terms are usually called

the coupling functions between units j and i . The coupling function can be implemented as either step functions [29] or smooth functions [22] of time since last spike. The use of step function requires less assumption, while the variance of estimator can be reduced by applying the smoothness constraint.

Because the neuronal networks are sparse, even in the neighboring neurons in the cerebral cortex, the probability of connection is only about ten percent ([30] and references therein). Thus sparsity should be considered for the inference of functional connectivity.

2.2.3 Predictability and causality

Point process GLM framework provides a natural measure for functional connectivity between two neurons, i.e. whether one neuron's spiking history can improve the prediction of another neuron's spiking event [10]. In these models, the log firing rate was modelled as a linear combination of contributions from different components, and fitted according to the point process GLM framework as will be described in the next section. Receiver Operating Characteristic (ROC) curves is commonly used to measure the how one process help predicting another [31]. The Area under the ROC curve (AUC) is a most widely used one number summary about ROC curve.

Because the synaptic connection between two neurons is directional, and the information flow is also directional: the upstream neuron send out information through synapses, and the downstream neuron acts according to the received information. It seems natural to interpret the association between neurons causally. In statistics, Granger causality describes the prediction power of one time series from others [32]. Despite its name, Granger causality does not represent the real causality. The concept has been used extensively in econometrics or imaging data of neuroscience, but its use in point processes models were limited. In one example the multiple spike train data were modelled as multivariate autoregressive model [32], and Granger causality was estimated.

2.3 Functional connectivity and graphical models

2.3.1 Graphical models and partial correlation

A graphical model is a probabilistic model for which a graph denotes the conditional independence structure between random variables. Undirected graph encodes the conditional dependency relationship between two nodes (nodes $A|B|\{others\}$) is equivalent to no edge between nodes A and B in the graph). A simple probabilistic graphical model is multivariate Gaussian, where the conditional independence

relationship is reflected in the zero value in the inversion covariance matrix (a.k.a precision matrix).

Whereas traditionally correlation and coherence were used to describe the association between the neurons, partial correlation or partial coherence are used to describe the conditional association between two neurons, i.e. the association between two neurons when the effects of all other observed neurons are removed. Partial correlation and partial coherence has been used to establish the connection between neurons [33, 34, 35] nonparametrically.

2.3.2 Inference of functional connectivity with graphical model

Graphical models and Bayesian network methods provide an intuitive methods to study functional connectivity between neurons [12]. The probabilistic graphical models are widely used in the machine learning community, and the use of these methods in neuronal network would be straight forward. It has been shown that the inference of functional connectivity can be faster than point process GLM models without much loss in reliability [14].

Shalizi proposed to infer a series of “hidden” states named *causal states* [36] to represent each node, which was successfully used in specifying refractory period and bursting behavior of neurons [37]. The method has been used to infer cluster of functionally related neurons in oscillating hippocampus neurons [38]. The method based on the *causal state* models may help us to decrease the computational cost further as it is one type of hidden markov model with the number of hidden states being minimal.

3 Data

The data used in this study was recorded from multielectrode array recordings of extracellular signals from the V1 area of the cortex. It has been showed that the quality of data from the arrays are comparable with single electrode thus can be used for further analysis [39].

In the recording, the Cyberkinetics “Utah” array (Blackrock Microsystems, Salt Lake City, Utah) was used. The device is a 10x10 grid of 1mm deep silicon microelectrodes spaced at 0.4 mm. The whole array covers an area of 12.96 mm^2 . The data was collected from anesthetized, paralyzed macaque monkeys (M fascicularis). Eye movement of the animal was minimized by continuous intravenous infusion of vecuronium bromide, and the pupils were dilated with topical atropine and the corneas protected with gas-permeable hard contact lenses. Data were collected while a short movies are played as stimuli. The stimuli include Gaussian

white noise, grating patterns with various orientation, as well as a short natural movie. The original recordings were processed by Kelly [40] for spike sorting. After processing, 105-129 candidate neural units were obtained from the 3 array implants, and roughly half of them are well isolated single units with quality comparable to single microelectrode recordings.

4 Methods

4.1 Simulating network of interacting neurons

Three-unit networks with different topologies are simulated and fitted. For each topology, the following procedure was performed to simulate the spike trains based on the coupling function.

1. Set the base firing rate, coupling strength, and coupling function shape.
2. Write out the conditional intensity function for each unit, where $H(t)$ only take the past 100 ms into consideration.

$$\log \lambda_i(t|H(t)) = \log \lambda_{i0} + h_i(t|H(t)) + \sum_{j \neq i} f_{ji}(t|H(t)) + s_i(x(t))$$

3. Loop through each time point t , and each unit i
 - Obtain the firing rate $\lambda_i(t)$ of each unit at time t .
 - Generate spike with probability $\lambda_i(t)\Delta$, where Δ is the time bin width.
 - Update the firing rate after time t .

4.2 Model fitting

As described before, the spike trains were modelled as interacting point processes. By assumption, the spiking of different neurons are conditionally independent given the history of the ensemble. Thus the model can be fitted separately for the spike train of each individual neuron as the dependent variable, and ensemble history being used as the independent variable. Ensemble history terms were obtained by convolution of the basis function sets with the spiking history of each neuron in the last 100 ms.

Poisson regression was performed using the *glmfit* procedure in Matlab software package based on iteratively reweighted least square algorithm. The fitted parameters were obtained from the fitting results, and the coupling function can be obtained by taking the product of basis functions and the fitted parameters.

4.3 ROC curve and AUC calculation

The prediction of spike based on kinematics information can be considered as a classification problem, e.g. given the kinematics information, whether the neuron spikes or not. ROC curve is used to assess the sensitivity and specificity of a classifier, but sometime we would like a one-number summary of the curve, and area under curve (AUC) is usually chosen. The ROC curve from different models were obtained using the standard method [31]. To get one point on the ROC , first choose a threshold $t \in (0, 1)$, and obtain prediction \hat{y}_i by setting the \hat{y}_i to 0 when $\hat{p}_i \leq t$ and 1 when $\hat{p}_i > t$. Then the true positive rate (sensitivity) is:

$$TPR(t) = \frac{\sum_i \hat{y}_i y_i}{\sum_i y_i} = \frac{\# \text{ bins with spikes predicted correctly}}{\# \text{ bins with spikes in real data}}$$

and the false positive rate (1-specificity):

$$FPR(t) = \frac{\sum_i \hat{y}_i (1 - y_i)}{N - \sum_i y_i} = \frac{\# \text{ bins with spike predicted but not in real data}}{\# \text{ bins with no spike in real data}}$$

4.4 Confidence band for the fitted coupling functions

Parametric bootstrap is used to obtain the confidence band of the fitted coupling functions. After the model was fitted, the estimation of the coupling function can be obtained from the basis set used for fitting and the estimated parameters. Bootstrap samples of networks can be obtained by simulating new network data from the estimated coupling functions, and fitted to obtain samples of coupling functions. A 95% confidence band of the coupling function is obtained by taking the pointwise 2.5% and 97.5% quantiles.

4.5 Significance of coupling by likelihood ratio test

When two models are nested, likelihood ratio test can be used to assess whether the more complex model is significantly better than the other one or not. To perform the test, the two models were both fitted and the corresponding likelihoods were calculated based on the fitted optimal parameters. For two models \mathcal{M}_1 and \mathcal{M}_2 with number of parameters $p_2 < p_2$, and \mathcal{M}_1 is nested in \mathcal{M}_2 , the likelihood ratio test reject H_0 when

$$L_2/L_1 > c$$

for some number c .

There are two different ways to obtain the right number c . First, the theoretical distribution of log likelihood ratio is χ_2 with degrees of freedom $p_2 - p_1$, thus we can obtain the c value by the CDF of χ_2 distribution.

Another method uses parametric bootstrap. The data is first fitted with the smaller model \mathcal{M}_1 , and all parameters are being estimated. Then simulate bootstrap network samples from the model, and fit for both \mathcal{M}_1 and \mathcal{M}_2 , so that the bootstrap samples of the log likelihood ratio are obtained. Then compare the original estimate with the empirical CDF of the log likelihood ratio. In the test of simulated data, there is almost no difference between the two methods of testing.

5 Results

Networks of three units are simulated to validate the methods used in the study. A three-unit network can be viewed as minimal in validating the methods, because it is the smallest possible network can be used to assess the indirect interaction, and different kinds of dependency relationships can be modelled with this type of network.

When direct feedback interaction (A->B and B->A exist at the same time) is excluded, all possible topologies of three-unit networks include:

- {A,B,C}, i.e. all units are independent.
- {A->B,C}, i.e. one edge
- {A->B,A->C}, i.e. one unit to two units
- {A->B,B->C}
- {A->B,C->B}
- {A->B,B->C,C->A}
- {A->B,B->C,A->C}

All other configurations can be obtained by permutating the labels.

Simulation and fitting of all these topologies were performed with similar results, thus only results from one topology (A->B->C) are reported below.

5.1 The simulated components and fitting results

The model for the simulation of the topology A->B->C is:

$$\log \lambda_A(t) = \log \lambda_{A0} + \int_{t-100}^t f_{AA}(s) dN_A(t-100+s)$$

$$\log \lambda_B(t) = \log \lambda_{B0} + \int_{t-100}^t f_{BB}(s) dN_B(t-100+s) + \int_{t-100}^t f_{AB}(s) dN_A(t-100+s)$$

$$\log \lambda_C(t) = \log \lambda_{C0} + \int_{t-100}^t f_{CC}(s) dN_C(t-100+s) + \int_{t-100}^t f_{BC}(s) dN_B(t-100+s)$$

Where $\lambda_A(t)$ represents the firing rate at time t , f_{AA} represents the history effect to the firing rate, and f_{AB} represents the the functions describes effect of spiking history of neuron A on neuron B . The spiking history and ensemble effects diminish after 100 ms.

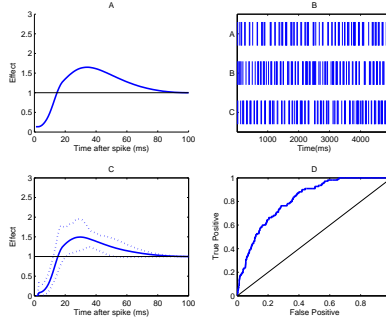


Figure 1: Simulation of a three-unit network (units A->B->C). A: The ensemble effect term (coupling function) used in simulation; B: The raster plot of one 5-second simulation; C: The fitted coupling function from A->B, and the 95% confidence band of the fitted function; D: The ROC curve for the prediction of spikes of unit B.

Figure 1 shows a simulated three-unit network and the fitting results. The base firing rate used in the simulation is around 40 Hz, which is the typical firing rate of an active neuron in the primary motor cortex (M1). The fitting process recovered the true coupling function in this setting, and the fitting is significant as indicated by the 95% confidence band obtained from parametric bootstrapping.

5.2 Sample size effects

Figure 2 shows the performance of the current inference method when the sample size changes. To better illustrate the change, a lower base firing rate (10 Hz) was used in the simulation. The distribution of the p-values was obtained by repeating the simulation-fitting process for 100 times. If the connectivity term is significant, the p -value should concentrate on the left (low) end of the x -axis. It is clear that when the sample size is small, the connection is not statistically significant. When the sample size become larger (10 seconds, corresponds to about 100 spikes here), more than 80% of the samples have p -value less than 0.1. Same information can be obtained from the confidence band on the bottom, when the sample size is small,

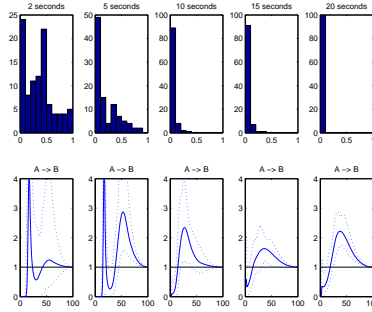


Figure 2: Sample size effect on inference of connectivity. Top: the distribution of p-values when the significance of the A->B connectivity was tested; Bottom: The fitted coupling function with its 95% confidence band. The plots show the results from 2s, 5s, 10s, 15s and 20s samples from left to right.

the horizontal line $y = 1$ is covered by the confidence band, which means that the coupling effect is insignificant. When the sample size is more than 10 seconds, we will see the significance of the connection.

Another way of looking at sample size effect on inference is the power. The testing powers when using 0.05 as the significance criteria are 0.15, 0.38, 0.75, 0.86 and 0.99 respectively for the sample sizes 2, 5, 10, 15, and 20 seconds.

5.3 Coupling Strength

The effect of coupling strength on functional connectivity inference was assessed by varying the amplitude of the coupling function α while keeping the shape of the coupling function unchanged, the model is:

$$\log \lambda_B(t) = \log \lambda_{B0} + \int_{t-100}^t f_{BB}(s) dN_B(t-100+s) + \int_{t-100}^t \alpha f_{AB}(s) dN_A(t-100+s)$$

Figure 3 shows that when the same sample size was used, the interaction term became more significant when the coupling strength become stronger. This result is expected, and it implies that much higher sample size is needed to infer the functional connectivity correctly when the coupling between neurons is weak.

5.4 Basis

Two most commonly used models for the coupling functions are step functions [29] and smooth function based on raised cosine basis [9, 22]. [9] proposed that a

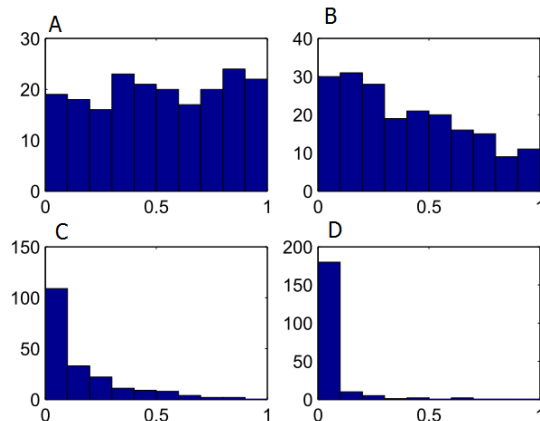


Figure 3: Effect of Coupling Strength on Inference. P value distribution from four different coupling strength α being used in the simulation: A. 0.1, B. 0.2, C. 0.4 and D. 0.8.

raised cosine basis set that has the following advantages: (1) it can represent the fine temporal structure near the time of spike, while constrained to be smooth in longer time scale; (2) the basis vectors sum to 1, such that the representation of the functions is phase invariant. In Figure 4, the fitting results from raised cosine basis and cosine basis are plotted. In both cases, five basis functions were used in the fitting covering 100 ms time scale. It is clear that the fitting from the two basis provided similar information and lead to same conclusion.

However there are still differences between the two fitting results. First, when the raised cosine basis was used, the effect to the spiking rate was constrained to diminish with time. While the step function did not impose such constraint. Another difference exists in the confidence band, the fitted smooth coupling function has narrower band (smaller variance) than the step function.

6 Proposed Research

6.1 Statistical details of point process GLM framework in functional connectivity inference

In the preliminary results, three-neuron networks were simulated and the effect of sample size, coupling strength and basis function were studied. The following work need to be done to finish the project.

First, I need to interpret the models and results both statistically and physio-

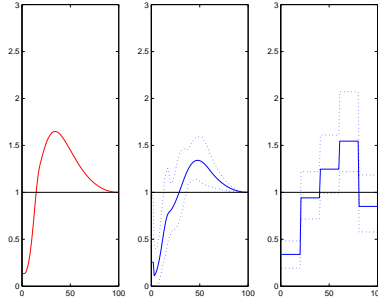


Figure 4: Inference with different basis functions. Left: the true coupling function; middle: fitted coupling function with raised cosine basis; right: fitted coupling function with step function. The fitting from step function basis is similar to the raised cosine basis, but with higher variance.

logically. To be specific, the coupling strength between two neurons need to be represented as how much the firing rate of one neuron being affected by another, and how the coupling strength difference affects the power of significance of the tests in my setting.

Secondly, since the number of neurons being recorded simultaneous will increase at fast rate, it is desirable to study the effect of these factors when the network is large. In the proposed work, large networks with dozens or more than hundred neurons will be simulated with different settings. The simulated data will be fitted and the effect of different settings will be assessed.

There are two challenges in this study. First the computational cost will be high when parametric bootstrapping is used for test. The solution is to rewrite my code using C++ and at the same time parallelize the process. The second challenge is that sparsity need to be considered especially when the sample size is small. I plan to implement the coordinate descent algorithm by Friedman et.al. [41] because it has good performance and flexibility.

6.2 Inference of conditional dependency and graphical models

Partial correlation or partial coherence will be used as a measure for conditional dependency. The proposed work include the following two steps.

First, study estimation and testing of partial correlation, including sample size considerations for normal data and binary data with ordinary Pearson-type partial correlation. Sparse estimation will be part of the project, but here the penalty will be on variables that are being partialled out, rather than on variables of interest.

Second, for point process data, Brillinger [33] pointed out that for a n -dimensional

multivariate point process $(\mathbf{X}_1, \mathbf{X}_2, \dots, \mathbf{X}_n)$, if we have

$$dN_1(t) = \left[\sum_{j=3}^n \int a_j(t-s) dN_j(s) \right] + d\Gamma_1(t)$$

$$dN_2(t) = \left[\sum_{j=3}^n \int a_j(t-s) dN_j(s) \right] + d\Gamma_2(t)$$

where Γ_1 and Γ_2 being noise processes with zero conditional expected value, and

$$\text{cov}(d\Gamma_1(s), d\Gamma_2(t)) = 0$$

then the partial coherence of X_1 and X_2 will be zero.

Once I have a suitable measure for the conditional dependency, again I will check the reliability of inference with regards to sample size, connection strength and different basis sets.

If time allows, after one set of conditional dependency relationships being inferred, some work will be done to infer a graph that is an Independence map for the set of dependency relationships [42].

7 Proposed Timeline

My proposed timeline is:

- Feb 2011 to Apr 2011: Coding and result analysis for the three-network simulation study.
- May 2011 to Jun 2011: Coding and result analysis for large network simulation study.
- Jul 2011 to Oct 2011: Partial correlation analysis for normal data, binary data and point process data. Apply the analysis to real data.
- Nov 2011 to Dec 2011: Writing the thesis.

References

- [1] Ian H Stevenson and Konrad P Kording. How advances in neural recording affect data analysis. *Nature neuroscience*, Unpublishe, 2011.

- [2] Emery N Brown, Robert E Kass, and Partha P Mitra. Multiple neural spike train data analysis: state-of-the-art and future challenges. *Nature neuroscience*, 7(5):456–61, May 2004.
- [3] Olaf Sporns. Brain connectivity. *Scholarpedia*, 2(10):4695, 2007.
- [4] James R Cavanaugh, Wyeth Bair, and J Anthony Movshon. Nature and interaction of signals from the receptive field center and surround in macaque V1 neurons. *Journal of neurophysiology*, 88(5):2530–46, November 2002.
- [5] Ian Nauhaus, Laura Busse, Matteo Carandini, and Dario L Ringach. Stimulus contrast modulates functional connectivity in visual cortex. *Nature neuroscience*, 12(1):70–6, January 2009.
- [6] Mehdi Aghagolzadeh, Seif Eldawlatly, and Karim G Oweiss. Identifying functional connectivity of motor neuronal ensembles improves the performance of population decoders. In *Neural Engineering, 2009. NER'09. 4th International IEEE/EMBS Conference on*, number 3, pages 534–537. IEEE, April 2009.
- [7] D H Perkel, G L Gerstein, and G P Moore. Neuronal spike trains and stochastic point processes. II. Simultaneous spike trains. *Biophysical journal*, 7(4):419–40, July 1967.
- [8] G L Gerstein and D H Perkel. Simultaneously recorded trains of action potentials: analysis and functional interpretation. *Science (New York, NY)*, 164(881):828, 1969.
- [9] Jonathan W Pillow, Liam Paninski, Valerie J Uzzell, Eero P Simoncelli, and E J Chichilnisky. Prediction and decoding of retinal ganglion cell responses with a probabilistic spiking model. *The Journal of neuroscience : the official journal of the Society for Neuroscience*, 25(47):11003–13, November 2005.
- [10] Wilson Truccolo, Uri T Eden, Matthew R Fellows, John P Donoghue, and Emery N Brown. A point process framework for relating neural spiking activity to spiking history, neural ensemble, and extrinsic covariate effects. *Journal of neurophysiology*, 93(2):1074–89, February 2005.
- [11] Jayant E Kulkarni and Liam Paninski. Common-input models for multiple neural spike-train data. *Network (Bristol, England)*, 18(4):375–407, December 2007.

- [12] Ed Bullmore and Olaf Sporns. Complex brain networks: graph theoretical analysis of structural and functional systems. *Nature reviews. Neuroscience*, 10(3):186–98, March 2009.
- [13] Seif Eldawlatly, Rong Jin, and Karim G Oweiss. Identifying functional connectivity in large-scale neural ensemble recordings: a multiscale data mining approach. *Neural computation*, 21(2):450–77, March 2009.
- [14] Seif Eldawlatly, Yang Zhou, Rong Jin, and Karim G Oweiss. On the use of dynamic Bayesian networks in reconstructing functional neuronal networks from spike train ensembles. *Neural computation*, 22(1):158–89, January 2010.
- [15] Michael Vidne, Jayant Kulkarni, Yashar Ahmadian, Jonathan W Pillow, Jonathon Shlens, E J Chichilnisky, E. Simoncelli, and Liam Paninski. Inferring functional connectivity in an ensemble of retinal ganglion cells sharing a common input. In *Frontiers in Systems Neuroscience. Conference Abstract: Computational and systems neuroscience*, pages 1–33, 2009.
- [16] D Golomb and D Hansel. The number of synaptic inputs and the synchrony of large, sparse neuronal networks. *Neural computation*, 12(5):1095–139, May 2000.
- [17] Karl J. Friston. Functional and effective connectivity in neuroimaging: A synthesis. *Human Brain Mapping*, 2(1-2):56–78, 1994.
- [18] J.G. White, E. Southgate, JN Thomson, and S. Brenner. The structure of the nervous system of the nematode *Caenorhabditis elegans*. *Philosophical Transactions of the Royal Society of London. B, Biological Sciences*, 314(1165):1–340, November 1986.
- [19] Olaf Sporns, Giulio Tononi, and Rolf Kötter. The human connectome: A structural description of the human brain. *PLoS computational biology*, 1(4):e42, September 2005.
- [20] A. Aertsen and H. Preissl. *Dynamics of activity and connectivity in physiological neuronal networks*. 1991.
- [21] William Penny, Karl Friston, John Ashburner, Stefan Kiebel, and Thomas Nichols, editors. *Statistical Parametric Mapping: The Analysis of Functional Brain Images*. ACADEMIC PRESS, 2007.

- [22] Wilson Truccolo, Leigh R Hochberg, and John P Donoghue. Collective dynamics in human and monkey sensorimotor cortex: predicting single neuron spikes. *Nature Neuroscience*, 13(1):105–111, December 2009.
- [23] B Horwitz. The elusive concept of brain connectivity. *NeuroImage*, 19(2):466–470, June 2003.
- [24] AA Fingelkurts and S Kähkönen. Functional connectivity in the brain—is it an elusive concept? *Neuroscience & Biobehavioral Reviews*, 28(8):827–836, 2005.
- [25] D.R. Brillinger. The identification of point process systems. *The Annals of Probability*, 3(6):909–924, 1975.
- [26] E S Chornoboy, L P Schramm, and a F Karr. Maximum likelihood identification of neural point process systems. *Biological cybernetics*, 59(4-5):265–75, January 1988.
- [27] Daryl J. Daley and David Vere-Jones. *An Introduction to the Theory of Point Processes: Volume I: Elementary Theory and Methods*. Springer, 2nd edition, 2002.
- [28] Zhe Chen, D Putrino, S Ghosh, Riccardo Barbieri, and Emery N Brown. Statistical Inference for Assessing Functional Connectivity of Neuronal Ensembles with Sparse Spiking Data. *IEEE transactions on neural systems and rehabilitation engineering : a publication of the IEEE Engineering in Medicine and Biology Society*, XX(c):1–12, October 2010.
- [29] Mengyuan Zhao and Satish Iyengar. Nonconvergence in logistic and poisson models for neural spiking. *Neural computation*, 22(5):1231–44, May 2010.
- [30] Tao Hu and Dmitri B. Chklovskii. Reconstruction of Sparse Circuits Using Multi-neuronal Excitation (RESCUME). *ADVANCES IN NEURAL INFORMATION PROCESSING SYSTEMS*, 22:790–798, 2009.
- [31] T Fawcett. An introduction to ROC analysis. *Pattern Recognition Letters*, 27(8):861–874, June 2006.
- [32] Michael Krumin and Shy Shoham. Multivariate autoregressive modeling and granger causality analysis of multiple spike trains. *Computational Intelligence and Neuroscience*, 2010:doi:10.1155/2010/752428, January 2010.
- [33] D.R. Brillinger. Remarks concerning graphical models for time series and point processes. *Brazilian Review of Econometrics*, 16(1):1—23, 1996.

- [34] Rainer Dahlhaus, M Eichler, and J Sandkühler. Identification of synaptic connections in neural ensembles by graphical models. *Journal of neuroscience methods*, 77(1):93–107, November 1997.
- [35] Michael Eichler, Rainer Dahlhaus, and Jürgen Sandkühler. Partial correlation analysis for the identification of synaptic connections. *Biological cybernetics*, 89(4):289–302, October 2003.
- [36] CR Shalizi and KL Shalizi. Blind construction of optimal nonlinear recursive predictors for discrete sequences. *Proceedings of the 20th conference on Uncertainty in artificial intelligence*, pages 504—511, 2004.
- [37] Robert Haslinger, Kristina Lisa Klinkner, and Cosma Rohilla Shalizi. The computational structure of spike trains. *Neural computation*, 22(1):121–57, January 2010.
- [38] Cosma Rohilla Shalizi, M Camperi, and K Klinkner. Discovering functional communities in dynamical networks. *Statistical Network Analysis: Models, Issues, and New Directions*, 4503:140–157, 2007.
- [39] RC Kelly, Matthew a Smith, Jason M Samonds, Adam Kohn, a B Bonds, J Anthony Movshon, and Tai Sing Lee. Comparison of recordings from microelectrode arrays and single electrodes in the visual cortex. *The Journal of neuroscience : the official journal of the Society for Neuroscience*, 27(2):261–4, January 2007.
- [40] RC Kelly. *Statistical Modeling of Spiking Activity in Large Scale Neuronal Networks*. PhD thesis, Carnegie Mellon University, 2010.
- [41] Jerome Friedman, Trevor Hastie, and Rob Tibshirani. Regularization Paths for Generalized Linear Models via Coordinate Descent. *Journal of statistical software*, 33(1):1–22, January 2010.
- [42] Daphne Koller and Nir Friedman. *Probabilistic graphical models: principles and techniques*. MIT Press, 1st edition, 2009.